Eur. Phys. J. D **8**, 29–40 (2000)

THE EUROPEAN PHYSICAL JOURNAL D

EDP Sciences

3D dissipative motion of atoms in a strongly coupled driven cavity

M. Gangl[a] and H. Ritsch

Institut für Theoretische Physik, Universität Innsbruck, Technikerstr. 25, 6020 Innsbruck, Austria

Received 5 March 1999 and Received in final form 4 May 1999

Abstract. We develop quantum models for the combined external and internal motion of atoms in a strongly coupled driven cavity mode including the transverse degrees of freedom. Using a simplified Gaussian mode function we determine the parameter regimes and prospects of 3D cooling and confinement of one or two atoms in the cavity field. Analysing the field dynamics for slow atoms traversing the cavity, we show that the spectrum of the transmitted and spontaneously scattered light contains ample information on the motional dynamics of the atom and can be nicely used to investigate the cooling properties of the system. Including several atoms in the dynamics we show how motional correlations build up by the common interaction with the cavity field. This can be looked upon as collisions at far distance and can be monitored *via* the transmitted field dynamics.

PACS. 32.80.Pj Optical cooling of atoms; trapping – 42.50.Vk Mechanical effects of light on atoms, molecules, electrons, and ions – 42.50.Lc Quantum fluctuations, quantum noise, and quantum jumps

1 Introduction

With recent advances in optical cavity technology and laser cooling of neutral atoms, experimentalists can now reach the strong coupling limit of a single atom and a single optical field mode. The atom-field coupling strength g is much larger than the involved decay rates of the atom Γ and the field mode κ [1–3]. By slowing down the atom to velocities of only a few recoil momenta $\hbar k$ long interaction times can be achieved [3,4]. Hence similar to the microwave regime [5] almost ideal representations of the Jaynes-Cummings model [6], a paradigm of quantum optics, are available. In contrast to Rydberg atoms used in micromasers, in the optical domain atoms in their ground state can be used, so that there are no fundamental limitations from the atomic lifetimes. In addition the cavity photons can be directly detected outside the resonator. At the same time mechanical effects [7] of the intracavity fields (as *e.g.* photon recoil and optical potentials) on the atom get more important and influence the atomic trajectories in the cavity field eventually accelerating and heating the atom. The dynamics of course strongly depends on the detunings and pump strengths used. Interestingly even for less than a single photon inside the cavity on average, significant light forces are predicted close to resonance [8–11]. Some features of this interaction have also been experimentally observed [3]. In many cases this is rather unwanted as light induced heating rapidly expells the atom from the interaction region [12,13]. In contrast to this we have shown in some recent work, that under suitable conditions the combined atom-field dynamics can also be exploited to cool the atom and sometimes even trap it close at an antinode of the field mode, exactly where the atom-field coupling is maximal [10,11]. This allows very long effective interaction times with the strongest possible coupling.

So far most considerations, however, have been confined to a quasi 1D case, where the fields are approximated by simple plane waves and only the atomic motion parallel to the wave vector is investigated. As the cavities used experimentally are rather tiny and possess spherical mirrors, the actual field modes have a small transverse extension (waist) and cold atoms entering from the side predominatly move at almost right angle to the wave vector. In this work we now generalize the model to 3D using a Gaussian transverse mode profile. This allows us to thoroughly study the combined atom-field dynamics for slow atoms traversing the cavity from the side and check the conditions for which atoms could be slowed down and trapped at mode field maxima in 3D. Naturally a central point in this discussion concerns the coupling of radial and longitudinal motion, which in general are governed by very different time scales.

Of course, besides calculating the dynamics itself, a question of almost equal importance is to look for the possibility of observing and interpreting it. In the optical domain one has the advantage that the transmitted cavity field as well as the incoherently scattered photons can be directly observed and analysed. Hence one gets real time information on the coupled atom field dynamics,

[a] e-mail: mgangl@mungo.uibk.ac.at

which of course can also be used for feedback (see *e.g.* atomic juggling [14,15]). Going beyond previous work we now also calculate the spectral properties of the transmitted and scattered light and show that the spectrum directly relates to the cooling and trapping properties of the system.

As a further extension to previous work [11], we generalize the model to more than one atom. As both particles are coupled to the same mode, which they influence through their motion, the atoms will interact with each other and their motions get correlated. Hence the dynamics strongly deviates from independent atom models, where the effect of all atoms are just summed up to give a single effective atom of stronger coupling. From a different perspective this atom-atom coupling can be viewed as a toy model for dipole-dipole coupling and light induced collisions at far distance, avoiding the near distance divergencies and other problems of dipole-dipole coupling. This coupling to a common mode has also some surprising consequences for the combined internal atomic dynamics as it has been discussed previously in context with the superradiant laser [16,17] or the construction of quantum gates [18].

Effects of collective interactions between atoms and a high-Q cavity mode have also been investigated by Bonifacio *et al.* and Grynberg *et al.* [19,20] in the context of the collective atomic recoil laser (CARL). They show that in the regime of relativistic atomic motion such a system can be used as a generator of coherent radiation. However in our work we will deal exclusively with very slow (cold) atoms.

Let us further point out here that our considerations should also be relevant for the dynamics of ions in a linear trap with a high-Q cavity along the trap axis [21–23]. As the longitudinal confinement of the ions is rather weak, cavity induced forces could play a crucial role if one tries to reach the motional ground state.

2 Model

We consider a two-level atom of resonance frequency ω_0 and mass m interacting with a single damped cavity mode with frequency ω_c that is weakly pumped with an amplitude η. The cavity mode is coupled to a reservoir that accounts for the cavity losses κ. In addition the atom is coupled to the free-space modes not encompassed by the cavity resulting in a spontaneous decay rate Γ.

The master equation describing our system reads (in an interaction picture with respect to the pump-frequency ω_P)

$$\dot{\rho}(t) = -\frac{\mathrm{i}}{\hbar}[H,\rho(t)] - \kappa\left(a^\dagger a\rho(t) - 2a\rho(t)a^\dagger + \rho(t)a^\dagger a\right) - \Gamma\left(\sigma^\dagger\sigma^-\rho(t) - 2\sigma^-\rho(t)\sigma^\dagger + \rho(t)\sigma^\dagger\sigma^-\right)$$

with

$$H = -\hbar\Delta_c a^\dagger a - \hbar\Delta_a\sigma^\dagger\sigma^- + \hbar g(x)\left(\sigma^\dagger a + a^\dagger\sigma^-\right) - \mathrm{i}\hbar\eta\left(a - a^\dagger\right) \quad (1)$$

$\Delta_c = \omega_P - \omega_c$, $\Delta_a = \omega_P - \omega_0$.

Here a and $a^\dagger$ are the annihilation and creation operators of the cavity mode with commutation relation $[a,a^\dagger] = \mathbf{1}$ and σ^-,σ^+ denote the usual lowering and raising operators of the two-level atom. Furthermore $g(x)$ is the atom-cavity coupling depending on the atomic position. In the following we set $\hbar = 1$.

If the cavity is very weakly driven, we have at most one quantum of excitation in the system: either there is one photon in the cavity and the atom is in the ground state or there is no photon in the cavity and the atom is in the excited state. Therefore the relevant Hilbert-space is restricted to the 3 states $\{|g,0\rangle, |g,1\rangle, |e,0\rangle\}$ where $|g\rangle, |e\rangle$ denote the atomic ground and excited states and $|0\rangle, |1\rangle$ the states with zero and one photon in the cavity mode. It follows immediately that $\langle\sigma_z a\rangle = -\langle a\rangle$ and all expectation values factorize, *e.g.* $\langle a^\dagger a\rangle = \langle a^\dagger\rangle\langle a\rangle$.

By use of the master equation we obtain the following equations for the one-time expectation-values of the system operators in the Heisenberg picture:

$$\begin{aligned}\langle\dot{a}(t)\rangle &= (\mathrm{i}\Delta_c - \kappa)\langle a(t)\rangle - \mathrm{i}g(x)\langle\sigma^-(t)\rangle + \eta,\\ \langle\dot{\sigma}^-(t)\rangle &= (\mathrm{i}\Delta_a - \Gamma)\langle\sigma^-(t)\rangle - \mathrm{i}g(x)\langle a(t)\rangle.\end{aligned} \quad (2)$$

The coupling between atom and cavity is position-dependent, which is important to study the influence of atomic motion on the dynamics of our system. In the following we use a semiclassical approach insofar as the atomic position and velocity are not quantized and enter our equations in form of parameters only.

3 Motion of a single particle in a Gaussian mode: Good cavity limit

3.1 Longitudinal motion

In the limit of a very good cavity ($\kappa \ll \Gamma, g$) one can assume the internal atomic dynamics to be much faster than the cavity dynamics. Accordingly one replaces the atomic operators by their stationary values. By the standard procedure of adiabatic elimination of the excited atomic state we obtain the following equations in the good-cavity-limit (with $\langle a\rangle \equiv \alpha$ and p denoting the atomic momentum):

$$\begin{aligned}\dot{\alpha} &= \left(-\kappa - \gamma(x) + \mathrm{i}\Delta_c - \mathrm{i}U(x)\right)\alpha + \eta\\ \dot{p} &= -|\alpha|^2\frac{\mathrm{d}}{\mathrm{d}x}U(x)\\ \dot{x} &= \frac{p}{m}\end{aligned} \quad (3)$$

where

$$\begin{aligned}U(x) &= \frac{\Delta_a}{\Delta_a^2 + \Gamma^2}g^2(x) \equiv U_0 g^2(x),\\ \gamma(x) &= \frac{\Gamma}{\Delta_a^2 + \Gamma^2}g^2(x) \equiv \gamma_0 g^2(x).\end{aligned}$$

Note that this set of equations coincides with the dynamical equations for a classical massive point dipole moving

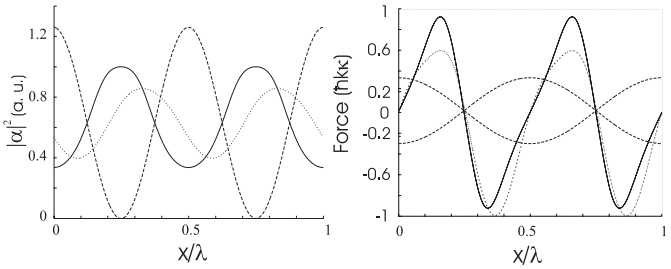

Fig. 1. Intracavity photonnumber (left picture) and force (right picture) exerted on an atom at rest (solid line) and at $v = 0.5\kappa/k$ respectively (dotted line) with $\Delta_a = 7\kappa$, $\Delta_c = 0\kappa$, $\kappa = \Gamma = 1\kappa$, $\eta = 1\kappa$, $g = 3\kappa$. For comparison we have also plotted the potential $U(x)$ (left picture) and the cavity standing-wave field (right picture) respectively (dashed lines).

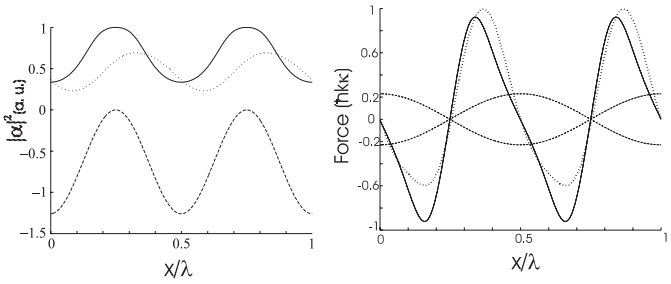

Fig. 2. Intracavity photonnumber (left picture) and force (right picture) exerted on an atom at rest (solid line) and at $v = 0.5\kappa/k$ respectively (dotted line) with $\Delta_a = -7\kappa$, $\Delta_c = 0\kappa$, $\kappa = \Gamma = 1$, $\eta = 1\kappa$, $g = 3\kappa$. For comparison we have also plotted the potential $U(x)$ (left picture) and the cavity standing-wave field (right picture) respectively (dashed lines).

in the cavity field, which we have derived in some previous work [11]. Clearly these equations can be easily generalised to three dimensions. Of course this model does not take into account momentum diffusion nor does it include friction forces as *e.g.* the Doppler cooling force.

Quite generally there are two limiting cases, for which the above approximations are valid:

- in the good-cavity-limit $g \gg \Gamma \gg \kappa$ we have two distinct time scales for the cavity and the atom respectively. As the lifetime of the upper atomic state is very small compared with the cavity lifetime the internal atomic degrees of freedom will adiabatically follow the local cavity field;
- similarily in the limit of a large detuning $|\Delta_a| \gg \Gamma, |\Delta_c|, g$ the atom is far away from resonance with the pump field and will not be excited significantly, so that the upperstate contribution to the atomic populations can be considered as a small perturbation.

The one dimensional dynamics described by these equations has been presented at some length in reference [11]. Nevertheless let us now briefly summarize some of the key physics contained in the above equations for the sake of comparison with the 3D model. From equation (3) it is easy to see the influence of the particle's position on the cavity field: on the one hand the field decay is enhanced *via* incoherent photon scattering at a rate $\gamma(x)$ and on the other hand the mode frequency is dispersively shifted through the induced atomic polarisation contained in the potential term $U(x)$. At the same time $U(x)$ represents the induced optical potential per photon for the atomic motion.

It is interesting to see that part of the induced friction force exerted on the atom can be understood from a purely classical argument connected to the strong dependence of the intracavity photon-number on the position of the atom within the cavity standing wave. Let us first look at the blue detuned case $\Delta_a > 0$ and $\Delta_c = 0$. Here the stationary intracavity photon-number has a maximum for the atom sitting at a node of the cavity standing-wave field, whereas the potential $U(x)$ possesses a minimum at the node (see Fig. 1). Assuming a particle slowly moving along the potential $U(x)$ one gets a certain delay in the

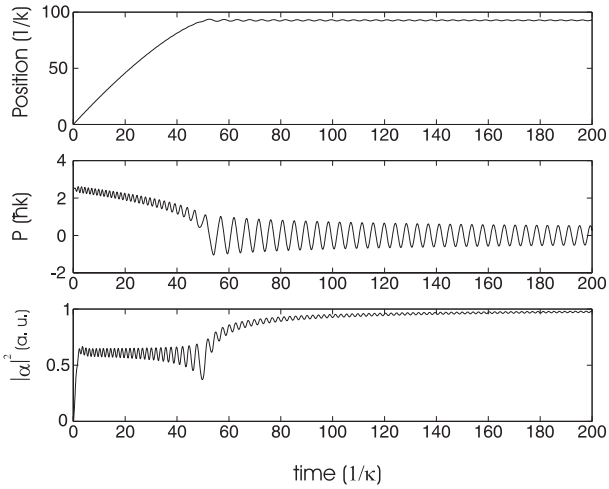

Fig. 3. Position (upper picture), momentum (middle) and intracavity photon-number for an atom starting at $v = 2.5\kappa/k$ with $\Delta_a = 7\kappa$, $\Delta_c = 0\kappa$, $\kappa = \Gamma = 1$, $\eta = 1\kappa$, $g = 3\kappa$ ($U_0 = 1.26\kappa$).

field dynamics with respect to the steady state and the maximum intracavity photon-number is reached after the particle has crossed the node and is moving uphill. Accordingly the particle sees a higher intracavity photon-number and thus a stronger deceleration when going up $U(x)$ than it sees when running down the potential $U(x)$ (see Fig. 1). Averaged over a wavelength this leads to a friction force. The particle is slowed down and finally trapped around a node of the field (see Fig. 3). Note the increase in the average intracavity intensity once the particle gets trapped in a single well directly showing the particle localisation.

The situation is of course reversed for red detuning $\Delta_a < 0$. As $\Delta_c = 0$ the intracavity photon-number still reaches a maximum for the atom at a node but now the potential $U(x)$ has a maximum there (see Fig. 2). If the particle is slowly moving this leads to an net acceleration of the atom on average.

This behaviour is again reversed if besides red atomic detuning the pump field is also red shifted with respect to the empty cavity resonance. Here the parameter region where the best cooling occurs lies around $\Delta_c \approx U_0$.

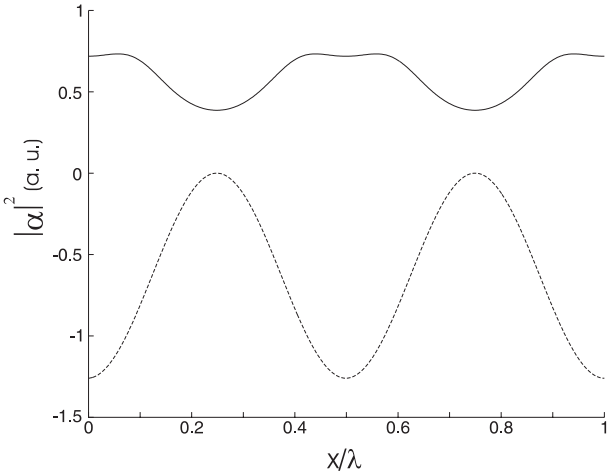

Fig. 4. Intracavity photonnumber for an atom at rest with $\Delta_a = -7\kappa$, $\Delta_c = -1.26\kappa$, $\kappa = \Gamma = 1$, $\eta = 1\kappa$, $g = 3\kappa$. For comparison we have also plotted the potential $U(x)$ (dashed line).

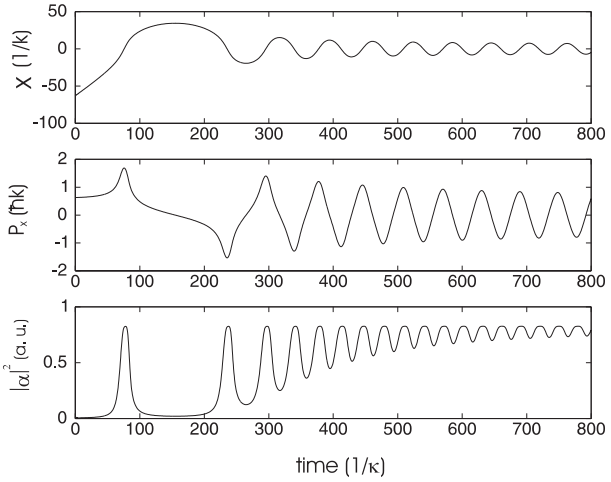

Fig. 5. Position perpendicular to the cavity axis (upper picture), momentum (middle) and intracavity photon-number for an atom moving along the transversal Gaussian profile with $U_0 = -15.2\kappa = \Delta_c$, $w_0 = 20\pi k^{-1}$ and $\gamma_0 = 0.1\kappa$.

In this case the intracavity photon-number reaches a maximum for the atom at an antinode of the field (see Fig. 4), which is also a potential minimum. In this case the atom will be trapped at the antinodes where the atom field coupling is maximal. As a difference to the blue detuned case the potential has also a minimum as far as the transverse motion is concerned yielding a 3D trap.

3.2 Full 3D motion in a Gaussian mode

We will now generalize equation (3) to 3 dimensions by using an approximative 3D-mode function $u_{nm}(x, y, z)$ and substituting $\mathrm{d}/\mathrm{d}x \rightarrow \nabla$. In the simplest case we use a approximated fundamental TEM_{00}-mode

$$u_{00}(x, y, z) = \cos(kz)\mathrm{e}^{-\frac{(x^2+y^2)}{w_0^2}}, \qquad (4)$$

where w_0 denotes the waist of the transverse Gaussian mode profile. We choose our coordinates such that the z-axis lies along the cavity and the x and the y-axis lie perpendicular to the cavity axis.

Of course it is only possible to transversely trap a particle perpendicular to the cavity axis by choosing red atomic detuning: $\Delta_a < 0$, $\Delta_c \approx U_0 < 0$ (see Fig. 5). Blue detuning would generate a radially repulsive potential hill. As a typical example shown in Figure 5, we demonstrate how a particle is transversely cooled and trapped. Every time it reaches the center of the cavity the intracavity photon-number gets maximal, since the atom shifts the cavity into resonance. As the atom is getting localized deeper in the potential, the intracavity photon-number approaches its steady state value.

In contrast to this behaviour in Figure 6 we have plotted the time-resolved intracavity photon-number for an atom traversing the cavity perpendicular to the cavity axis with a small velocity component along the standing wave and no detuning between cavity, atom and pump field.

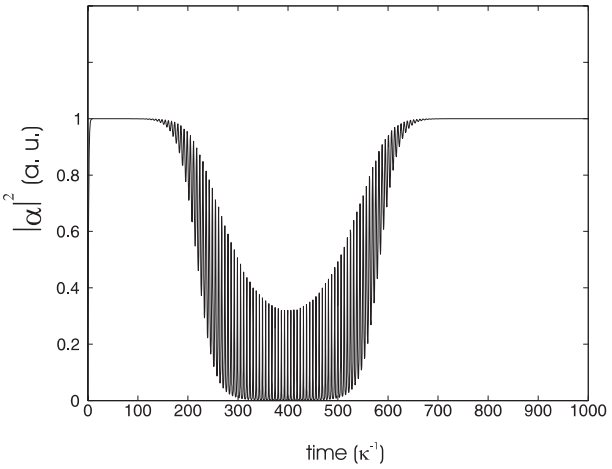

Fig. 6. Intracavity photon-number for an atom with $\Delta_a = \Delta_c = 0\kappa$, $g = 4\kappa$, $\eta = 1\kappa$, $w_0 = 200\pi k^{-1}$ and $\Gamma = 0.5\kappa$. $\mathbf{x} = (-2000, 0, 0)$, $\mathbf{p} = (5, 0, 0.5)$.

This is a typical choice of parameters used in experimental setups to detect the presence of atoms traversing the optical resonator [1,3]. Here we have no net force on the atom and the dominant effect of the atom is to scatter light out of the cavity field. One can nicely see the transversal Gaussian profile in the time-resolved intracavity photon-number as the atom crosses the cavity superimposed by the fast oscillations from the longitudinal standing wave structure.

In the following we show the dynamics of an atom with only a small component of the atomic velocity perpendicular to the cavity axis as it would arise in an experiment with very cold atoms (Figs. 7–10). For the chosen parameters the particle, which is initially unbound, is finally trapped. Note that at the time when the atom is trapped within a single potential well the intracavity photon-number increases to a higher mean value reflecting a stronger effective coupling. This is because the atom

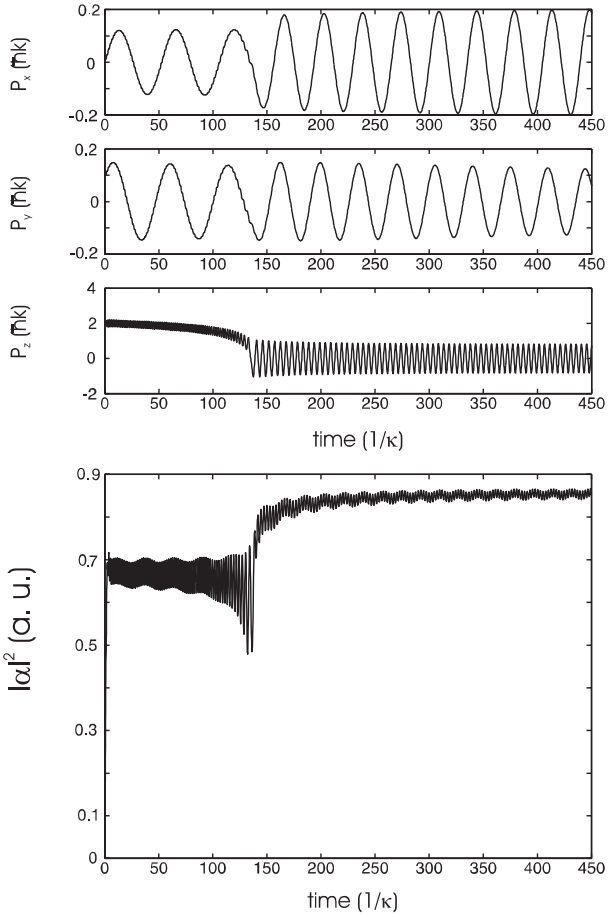

Fig. 7. Momentum components (upper picture) and intracavity photon-number for an atom moving along the longitudinal cosine with small velocity components along the transversal Gaussian profile. $U_0 = -1.2\kappa = \Delta_c$, $w_0 = 10k^{-1}$, $\gamma_0 = 0.07\kappa$, $\mathbf{x} = (-1, -1, 0)$, $\mathbf{p} = (0.01, 0.1, 2)$.

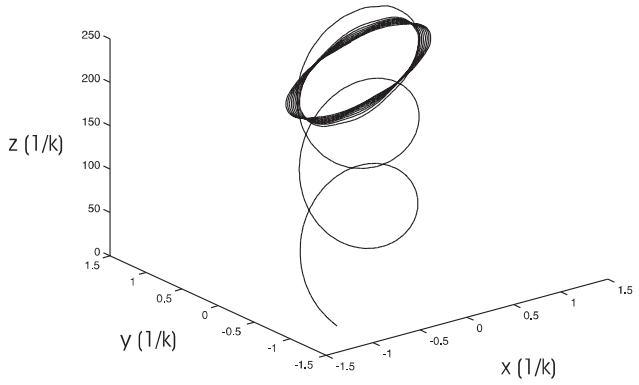

Fig. 8. 3D-position of the atom for the parameters of Figure 7. Starting at $z = 0$ the atom moves along the positive z-direction until it is longitudinally trapped within a single potential well in the cavity standing-wave field.

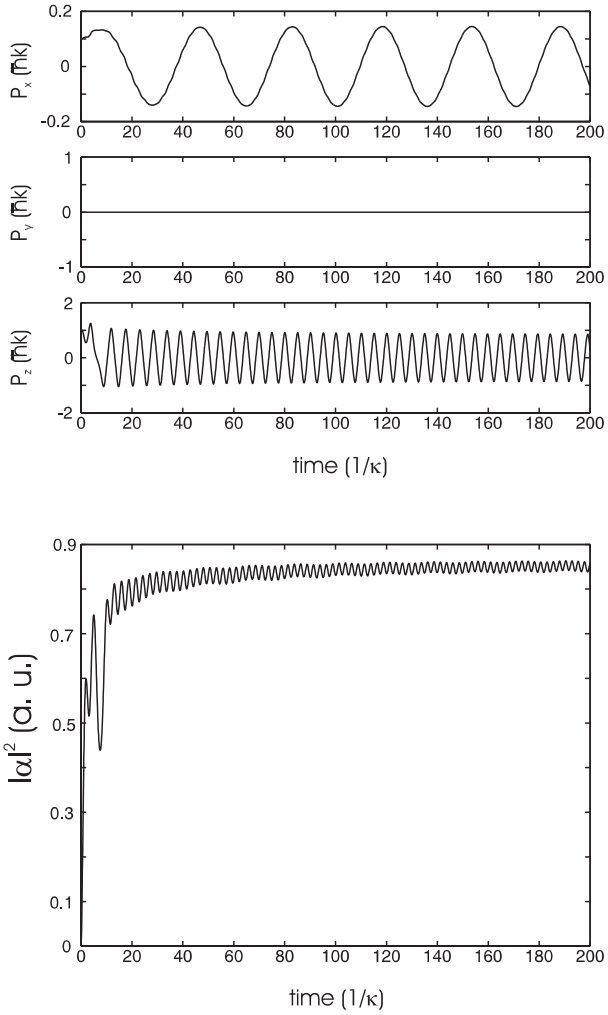

Fig. 9. Momentum components (upper picture) and intracavity photon-number for an atom moving along the longitudinal cosine with small velocity components along the transversal Gaussian profile. $U_0 = -1.2\kappa = \Delta_c$, $w_0 = 10k^{-1}$, $\gamma_0 = 0.07\kappa$, $\mathbf{x} = (-1, 0, 0)$, $\mathbf{p} = (0.1, 0, 1)$.

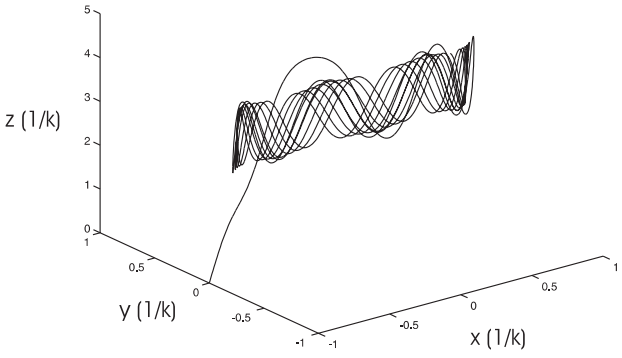

Fig. 10. 3D-position of the atom for the parameters of Figure 9.

oscillates only weakly around its equilibrium position at an antinode of the standing wave. Hence the cavity is pulled into resonance by the atom more effectively than by an atom, which moves along the standing wave and sees only a motion averaged smaller coupling. Note that the changes in the intracavity intensity reflect the fast z-axis oscillations as well as the slow transverse dynamics of the atom. This provides an experimental possibility of observing the trapping process. Alternatively in an experiment, where relatively fast atoms transversely cross the cavity at almost right angle, the effective coupling is different for red and blue detuning and directly reflects the longitudinal temperature of the atoms.

4 Coupled motion of two particles in a Gaussian mode

Obviously even in the case of less than one atom at a time in the cavity on average one has a finite probability of two atoms being present at the same time. For many experiments it is sufficient to just consider an effective atom with a coupling given by the sum of the two atomic couplings $g_{\text{eff}} = g(x_1) + g(x_2)$ instead [16,17]. Obviously in our type of setup such an approximation is completely useless and wrong. The combined dynamics shows a much richer and physically more interesting dynamics as we will show at some typical examples below. Starting from the simple equation (3) it is straightforward to increase the number of particles interacting with the cavity mode, which yields:

$$\begin{aligned} \dot{\alpha} &= (-\kappa - \gamma(\mathbf{x}_1) - \gamma(\mathbf{x}_2) + \mathrm{i}\Delta_c - \mathrm{i}U(\mathbf{x}_1) - \mathrm{i}U(\mathbf{x}_2))\,\alpha + \eta, \\ \dot{\mathbf{p}}_1 &= -|\alpha|^2 \nabla_1 U(\mathbf{x}_1), \quad \dot{\mathbf{p}}_2 = -|\alpha|^2 \nabla_2 U(\mathbf{x}_2), \\ \dot{\mathbf{x}}_1 &= \frac{\mathbf{p}_1}{m}, \quad \dot{\mathbf{x}}_2 = \frac{\mathbf{p}_2}{m}, \end{aligned} \tag{5}$$

where $\mathbf{x}_1$, $\mathbf{p}_1$, $\mathbf{x}_2$, $\mathbf{p}_2$ describe the positions and momenta of atom 1 and atom 2 respectively. As both particles interact with the same cavity field they interact with each other non-linearly and over a large distance *via* this field. As a consequence their motion gets strongly correlated. Figure 11 shows a situation where one atom moves along the z-axis and the other flies perpendicular to this axis. Both atoms are trapped for the chosen parameters of suitable red detuning so that the cavity is shifted into resonance due to the coupling with the atoms. Note that the intracavity photon-number of the transmitted light looks completely different compared to the one-atom situation of Figures 5 and 10. As atom 2 is trapped within one potential well of the longitudinal cosine the average intracavity photon-number increases. Hence atom 1 is accelerated to the center of the transversal Gaussian leading to an approximately exponential increase in the intracavity photon-number modulated by the fast cosine oscillations due to atom 2. In the one-atom case the intracavity photon-number would be highest for the atom approaching the center of the Gaussian profile. Due to the non-linear interactions between the atoms however we see a sudden drop in the intracavity photon-number.

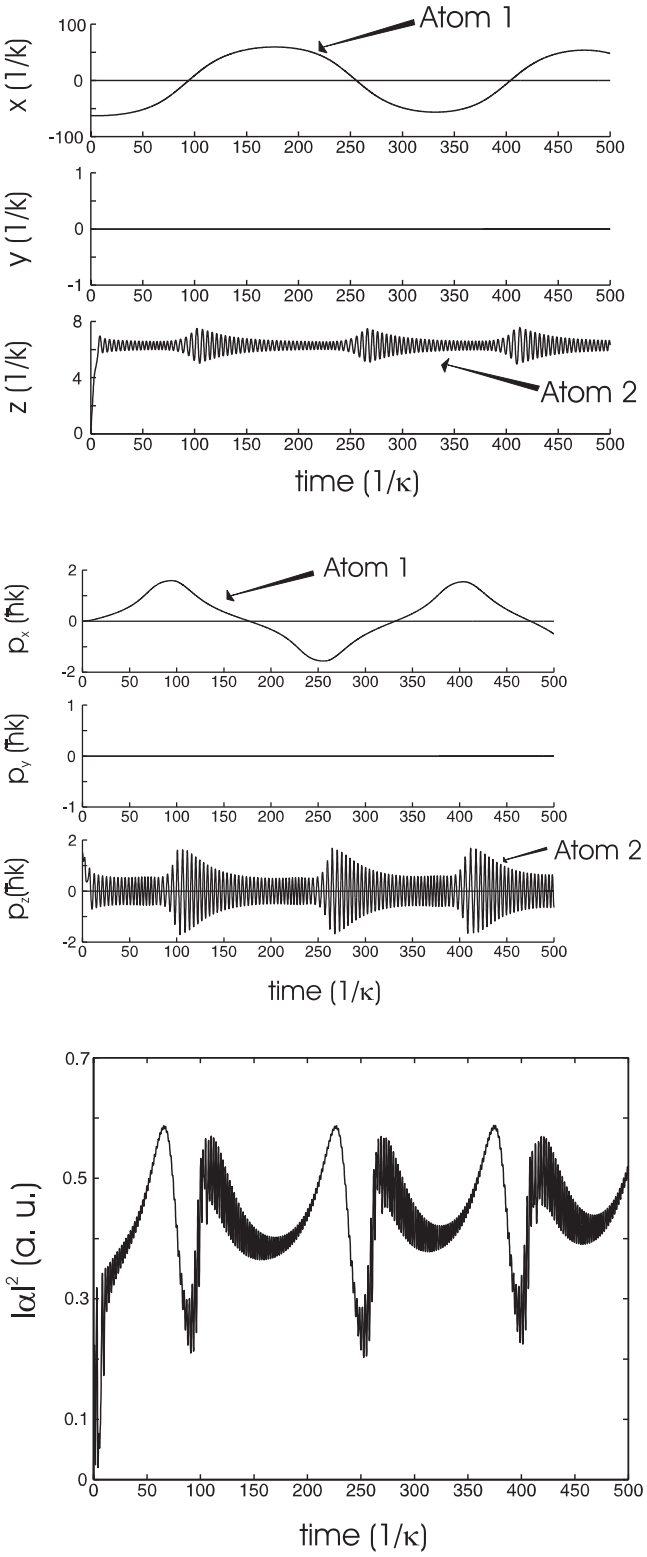

Fig. 11. Positions (upper picture), momenta (middle) and intracavity photon-number for two atoms. Atom 2 moving along the longitudinal cos and atom 1 moving along the transversal Gaussian profile. $\Delta_a = -15\kappa$, $w_0 = 20\pi k^{-1}$, $\gamma = \kappa = 1$, $\mathbf{x}_1 = (-20\pi, 0, 0)$, $\mathbf{x}_2 = (0, 0, 0)$, $\mathbf{p}_1 = (0, 0, 0)$, $\mathbf{p}_2 = (0, 0, 1.5)$.

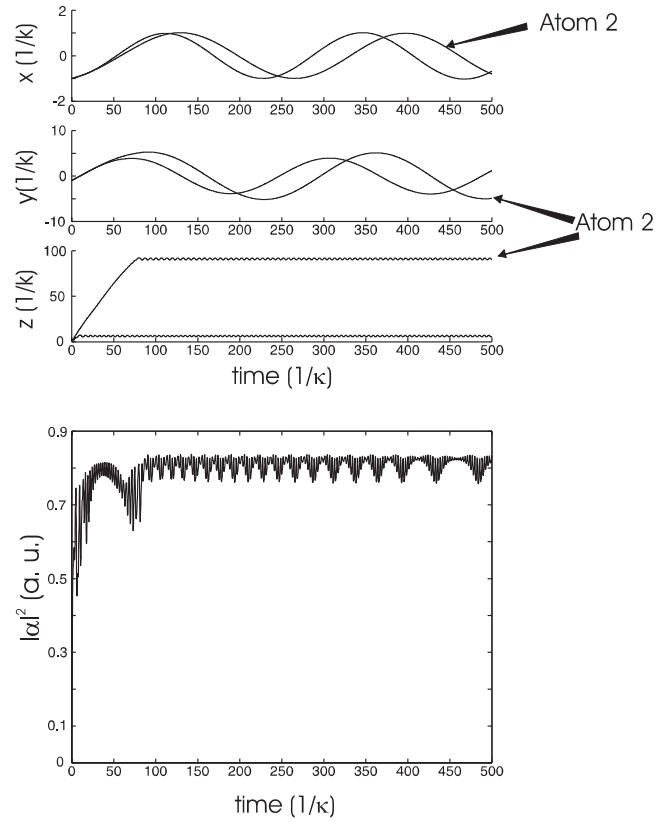

Fig. 12. Positions (upper picture) and intracavity photon-number for two atoms with $\Delta_\mathrm{a} = -15\kappa$, $w_0 = 20\pi k^{-1}$, $\gamma = \kappa = 1$, $\mathbf{x}_1 = (-1, -1, 0)$, $\mathbf{x}_2 = (-1, -1, 0.1)$, $\mathbf{p}_1 = (0.01, 0.1, 1)$, $\mathbf{p}_2 = (0.01, 0.1, 1.5)$.

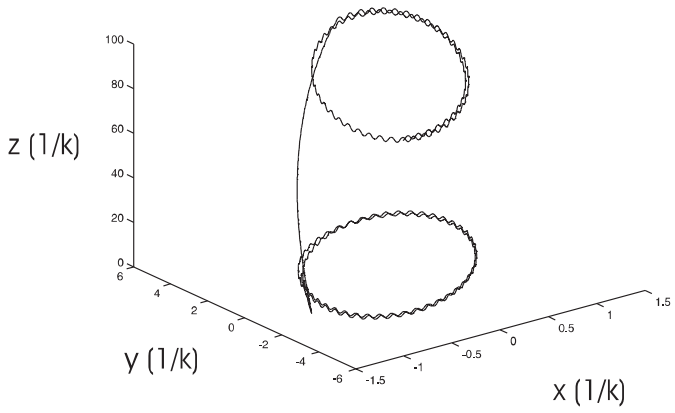

Fig. 13. 3D-position of atom 1 and atom 2 for the parameters of Figure 12. Both atoms are trapped in 3D.

As a second example in Figures 12 and 13 both atoms are chosen to have momentum mainly along the standing-wave axis with small transversal components. Again both atoms are trapped and the time-resolved intracavity photon-number reflects the complex interactions between the two atoms.

5 Light spectra for a moving atom in a standing wave

As we have seen in the previous section the intracavity and hence also the transmitted field contain significant information on the particle dynamics. Besides simply looking at the corresponding intracavity photon-number expectation values as a function of time, we will in the following analyse the transmitted light as well as the scattered light in more detail and calculate the corresponding spectra [24]. Of course, due to the relatively low number of scattered photons a direct observation of these spectra seems experimentally challenging, although the resonance fluorescence of single atoms and ions has been measured before [25]. To keep the analysis as simple as possible we return to the model, where the excited atomic state is not adiabatically eliminated and the whole system is only weakly excited.

Following standard procedures [26] we define the time-dependent spectrum of light by

$$S(\omega, T) = \frac{1}{T}\int_0^T \mathrm{d}t \int_0^T \mathrm{d}t' \mathrm{e}^{-\mathrm{i}\omega(t-t')}\langle E^{(-)}(t)E^{(+)}(t')\rangle, \tag{6}$$

where $E^{(+)}(t)$ is the positive-frequency part of the electric field strength and T is the integration time of the detector, which has to be chosen large enough in order to allow for a good resolution of the frequency components.

As mentioned before for a weakly driven cavity all expectation values factorize. This allows to calculate spectra simply in the following way

$$\begin{aligned} S_\mathrm{c}(\omega - \omega_\mathrm{P}, T) &= \mathcal{N}\frac{1}{T}\left|\int_0^T \mathrm{d}t \mathrm{e}^{\mathrm{i}(\omega-\omega_\mathrm{P})t}\langle a(t)\rangle\right|^2 \\ S_\mathrm{a}(\omega - \omega_\mathrm{P}, T) &= \mathcal{N}\frac{1}{T}\left|\int_0^T \mathrm{d}t \mathrm{e}^{\mathrm{i}(\omega-\omega_\mathrm{P})t}\langle \sigma^-(t)\rangle\right|^2, \end{aligned} \tag{7}$$

where $S_\mathrm{c}(\omega - \omega_\mathrm{P}, T)$ is the spectrum of the photons emitted through the cavity mirrors and $S_\mathrm{a}(\omega - \omega_\mathrm{P}, T)$ is the spectrum of the photons emitted out the sides of the cavity centered around the pump-frequency ω_P and observed at a time T. $\mathcal{N}$ is a normalization factor

$$\mathcal{N}^{-1} = \frac{2\pi}{T}\int_0^T \mathrm{d}t \left(|\langle a(t)\rangle|^2 + \left|\langle \sigma^-(t)\rangle\right|^2\right)$$

assuring that

$$\int_{-\infty}^{\infty} \mathrm{d}\omega'(S_\mathrm{c}(\omega', T) + S_\mathrm{a}(\omega', T)) = 1,$$

where $\omega' \equiv \omega - \omega_\mathrm{P}$ and we have used $\int_{-\infty}^{\infty}\mathrm{d}\omega' \mathrm{e}^{\mathrm{i}\omega' t} = 2\pi\delta(t)$.

For an atom at rest at an antinode of the standing wave we recover the well-known double-peaked spectrum located at the frequencies corresponding to the upper and the lower eigenenergy E_+, E_- of the two dressed

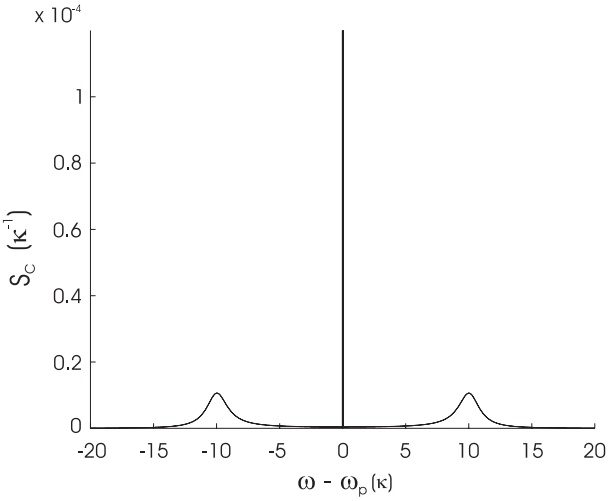

Fig. 14. Cavity spectrum for an atom at rest. $g = 10\kappa$, $\Delta_{\rm a} = \Delta_{\rm c} = 0\kappa$, $\Gamma = \kappa = 1$.

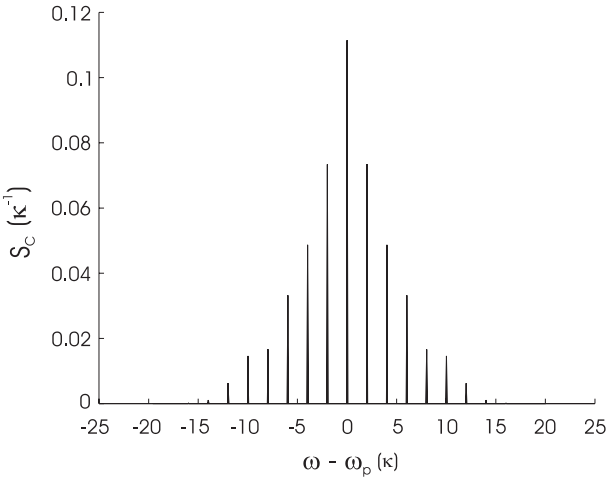

Fig. 15. Cavity spectrum for an atom with $v = 1\kappa/k$. $g = 10\kappa$, $\Delta_{\rm a} = \Delta_{\rm c} = 0\kappa$, $\Gamma = \kappa = 1$.

states [27] with one quantum of excitation plus a delta peak at $\omega = \omega_{\rm P}$ representing the pump (Fig. 14)

$$E_+ = -\Delta_{\rm c} - \frac{\Delta_{\rm a} - \Delta_{\rm c}}{2} + \frac{1}{2}\sqrt{(\Delta_{\rm a} - \Delta_{\rm c})^2 + 4g(x)^2},$$
$$E_- = -\Delta_{\rm c} - \frac{\Delta_{\rm a} - \Delta_{\rm c}}{2} - \frac{1}{2}\sqrt{(\Delta_{\rm a} - \Delta_{\rm c})^2 + 4g(x)^2}. \quad (8)$$

For a moving atom new peaks emerge in both the cavity and the atomic spectrum (Figs. 15 and 16). They can be assigned to velocity-induced modulation of the intracavity field and the occupation probability of the excited atomic state. When the initial transients causing the two-peaked spectrum have died out, this is the only remaining time-dependence in the system. A look at Figures 15 and 16 shows that peaks in the cavity spectrum $S_{\rm c}$ emerge at $\omega - \omega_{\rm P} = \pm 2nkv$ whereas peaks in the atomic spectrum $S_{\rm a}$ arise exclusively at $\omega - \omega_{\rm P} = \pm(2n+1)kv$ with $n = 0, 1, 2, ...$ Qualitatively this can be understood from the following argument.

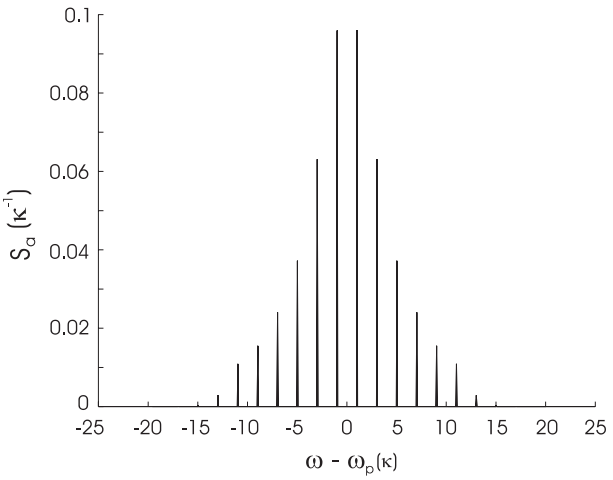

Fig. 16. Atomic spectrum for an atom with $v = 1\kappa/k$. $g = 10\kappa$, $\Delta_{\rm a} = \Delta_{\rm c} = 0\kappa$, $\Gamma = \kappa = 1$.

Due to the atomic motion, the process of photon emission by the atom is shifted from resonance with the initial pump frequency, with detuning $+kv$ if the emitted photon propagates in the same direction as the atom; it is shifted out of resonance by $-kv$ if the emitted photon propagates in the opposite direction to the atom. Similarily, the process of photon absorption is out of resonance with the atom with detuning $-kv$, if the absorbed photon propagates in the same direction as the atom; it is out of resonance with detuning $+kv$ if the absorbed photon propagates in the opposite direction to the atom. In the following we discuss the processes involving one photon exchange between cavity and atom at most:

(i) the photon enters the cavity and is absorbed by the atom after an *odd number* of mirror reflections, when the photon direction has been reversed. If it is finally transmitted after being emitted by the atom into the direction of atomic movement it will contribute to the peak at $\omega - \omega_{\rm P} = 2kv$. If it is transmitted after being emitted by the atom in the opposite direction to atomic movement it will contribute to the peak centered at $\omega - \omega_{\rm P} = 0$ in the cavity spectrum;

(ii) the photon enters the cavity and is absorbed by the atom after an *even number* of mirror reflections, when the photon is travelling in the same direction as the atom. If it is finally transmitted after being emitted by the atom into the direction of atomic movement it will contribute to the peak at $\omega - \omega_{\rm P} = 0$. If it is transmitted after being emitted by the atom in the opposite direction to atomic movement it will contribute to the peak at $\omega - \omega_{\rm P} = -2kv$;

(iii) the photon enters the cavity and is transmitted *without having been absorbed* by the atom. It will contribute to the central peak at $\omega - \omega_{\rm P} = 0$.

Peaks at higher multiples of $\pm 2kv$ can be explained by the contribution of processes involving more than one absorption-emission cycle between cavity mode and atom. If there is a non-zero detuning between cavity and atom

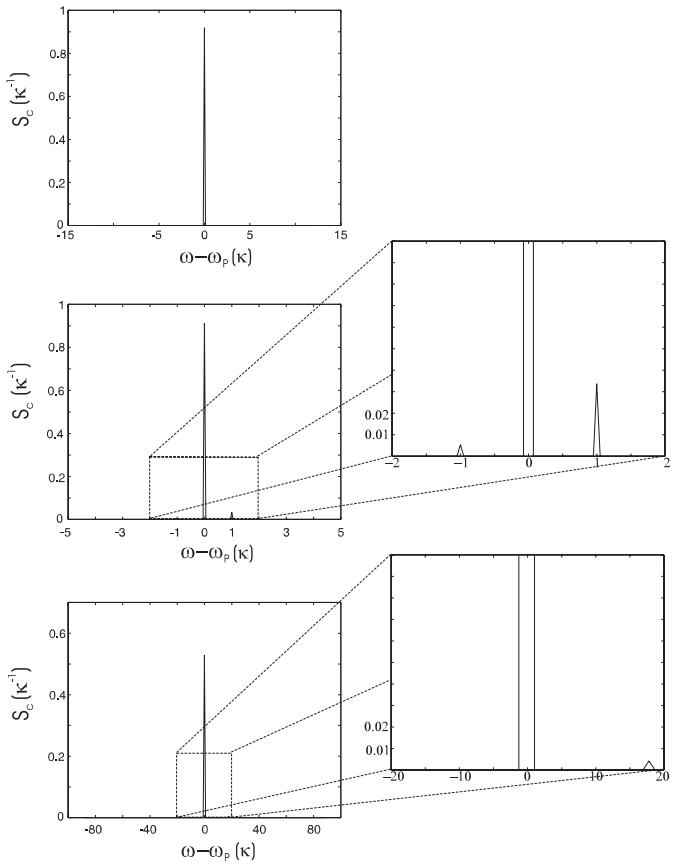

Fig. 17. Cavity spectra S_c for $v = 0\kappa/k$ (upper), $v = 0.5\kappa/k$ (middle) and $v = 8.9\kappa/k$. $\Delta_\mathrm{a} = -10\kappa$, $\Delta_\mathrm{c} = -2\kappa$, $g = 3\kappa$, $\Gamma = \kappa = 1$, $\eta = 0.1\kappa$.

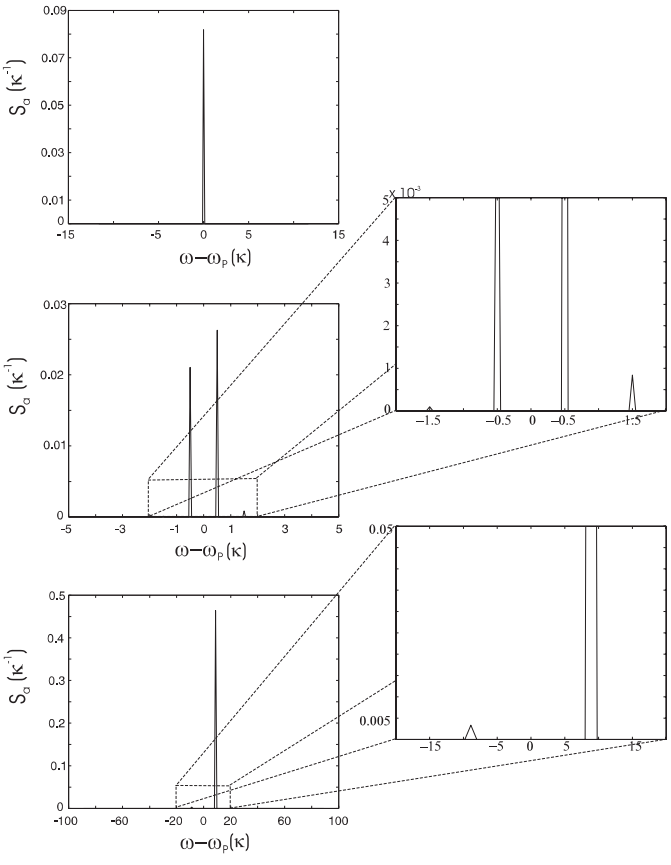

Fig. 18. Atomic spectra S_a for $v = 0\kappa/k$ (upper), $v = 0.5\kappa/k$ (middle) and $v = 8.9\kappa/k$. $\Delta_\mathrm{a} = -10\kappa$, $\Delta_\mathrm{c} = -2\kappa$, $g = 3\kappa$, $\Gamma = \kappa = 1$, $\eta = 0.1\kappa$.

photons will be absorbed preferably from one direction resulting in an asymmetry of the spectrum.

To understand the peaks at odd multiples of the first-order Doppler shift in S_a one has to note that for the photon contributing to the atomic spectrum it has to be emitted out the sides of the cavity, *i.e.* in our 1D model, perpendicular to the direction of atomic motion. Therefore there will be one Doppler shift less compared to the cavity spectrum resulting in peaks at $\omega - \omega_\mathrm{P} = \pm(2n+1)kv$, $n = 0, 1, 2, ...$ and the peak at $\omega - \omega_\mathrm{P} = 0$ is missing.

If we choose Δ_c or $\Delta_\mathrm{a} \neq 0$ there will be a force exerted on the atom (see our previous work). In this parameter regime we obtain asymmetrical spectra (Figs. 17–20). Note that there are less sidebands compared to Figures 15 and 16 because of the smaller g, which means that there are less photon exchanges between the atom and the cavity mode before the photon gets lost through either decay channel.

The coherent spectra hence contain ample information on the atom-field dynamics. Although some quantitative changes especially in the width of the existing peaks are expected, the qualitative behaviour of these spectra should remain even for stronger excitation (pumping) of the system, where a direct observation seems more feasible. In addition part of this information can also be extracted from the intensity correlations (power spectra) of the scattered light, which also shows sidebands.

6 Comparison between averaged force and integrated spectra

Naturally the kinetic energy lost or gained by the atom has to be transferred to the field in some way. An asymmetry in the spectra implies also a shift of the average energy of the involved photons. To check this presumption we compare the asymmetry in the spectra with the net force exerted on the atoms. In order to get numerical results for the spectral asymmetry, we have to compute the integrals

$$\Delta S_\mathrm{c}(\omega', T) = \int_{-\infty}^{\infty} \mathrm{d}\omega' \omega' S_\mathrm{c}(\omega', T),$$
$$\Delta S_\mathrm{a}(\omega', T) = \int_{-\infty}^{\infty} \mathrm{d}\omega' \omega' S_\mathrm{a}(\omega', T). \qquad (9)$$

We will speak of a blue-asymmetry if $\Delta S(\omega', T) > 0$ and of a red-asymmetry if $\Delta S(\omega', T) < 0$. In the situation of a blue-asymmetry the scattered light observed contains more energy than the light pumped into the cavity, whereas it is less energetical in the red-asymmetry case.

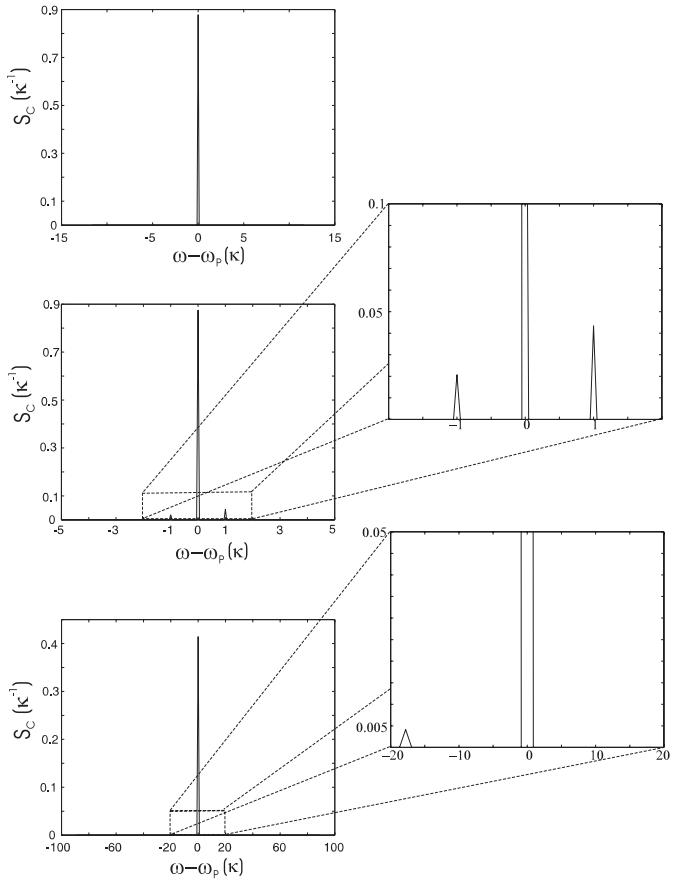

Fig. 19. Cavity spectra $S_{\rm c}$ for $v = 0\kappa/k$ (upper), $v = 0.5\kappa/k$ (middle) and $v = 8.9\kappa/k$. $\Delta_{\rm a} = 8\kappa$, $\Delta_{\rm c} = 0\kappa$ $g = 3\kappa$, $\Gamma = \kappa = 1$, $\eta = 0.1\kappa$.

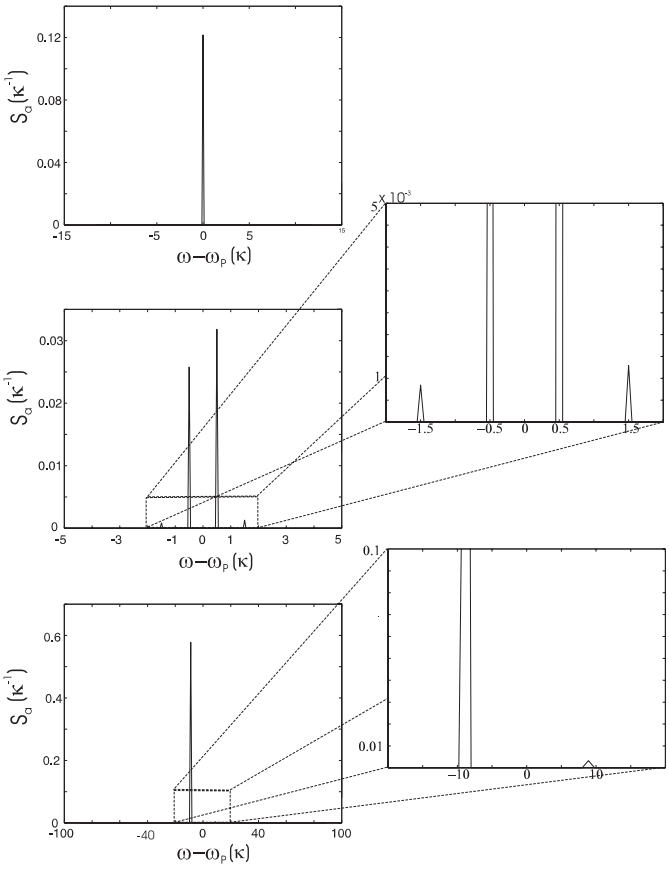

Fig. 20. Atomic spectra $S_{\rm a}$ for $v = 0\kappa/k$ (upper), $v = 0.5\kappa/k$ (middle) and $v = 8.9\kappa/k$. $\Delta_{\rm a} = 8\kappa$, $\Delta_{\rm c} = 0\kappa$, $g = 3\kappa$, $\Gamma = \kappa = 1$, $\eta = 0.1\kappa$.

In Figures 21 and 22 we compare these asymmetries with the forces averaged over one wavelength.

In Figure 21 there is a blue asymmetry in the cavity spectrum for small v related to a cooling force. As this friction force is cavity mediated there is no asymmetry in the atomic fluorescence spectrum. For intermediate velocities $kv/\kappa \approx 8$ the red asymmetry in the atomic spectrum is almost one magnitude of order larger than the asymmetry in $S_{\rm c}$. This allows to identify the heating force in this velocity range as directly related to the Doppler force.

In Figure 22 it can be seen that there is a blue asymmetry in the cavity spectrum, while there is no asymmetry in the atomic spectrum for the cavity mediated force. For $kv \approx \Delta_{\rm a}$ the cooling force is mainly Doppler mediated and accordingly we see a strong blue asymmetry in $S_{\rm a}$ and a negligible one in $S_{\rm c}$.

Hence this analysis gives us a direct access to the relative size of cavity mediated friction forces and free space Doppler cooling. Fortunately the results are in quite good agreement with the interpretation of the various force contributions, which we found in previous work [11].

7 Conclusions

We have shown that cooling and trapping a single particle in the fundamental TEM_{00} mode of a high-Q microscopic resonator seems possible using cold atoms and currently available cavity technology. The final temperature is only limited by the cavity finesse and can be much less than the Doppler limit and in principle be also smaller than the recoil limit. In particular the thermal kinetic energy can be much smaller than the well depth assuring long effective interaction times. The process of capturing and cooling the atom can be directly monitored from the transmitted cavity field. By analysing the spectral properties of this light one obtains even more detailed information on the ongoing system dynamics. For this even very weak intracavity fields of the order of one average photon in the mode can be used rendering this system to be a prototype tool to investigate quantum dynamics. This might also provide for a possibility to trap and cool small molecules with a strong enough dipole moment, without involving spontaneous emission and hence avoiding the need for a closed optical transition.

Let us further point out here, that in a realistic experimental situation one has to take into account gravity. To get some first estimate of its importance one has to compare the gravitational energy $E_{\rm g} = mg\Delta x$, which an atom

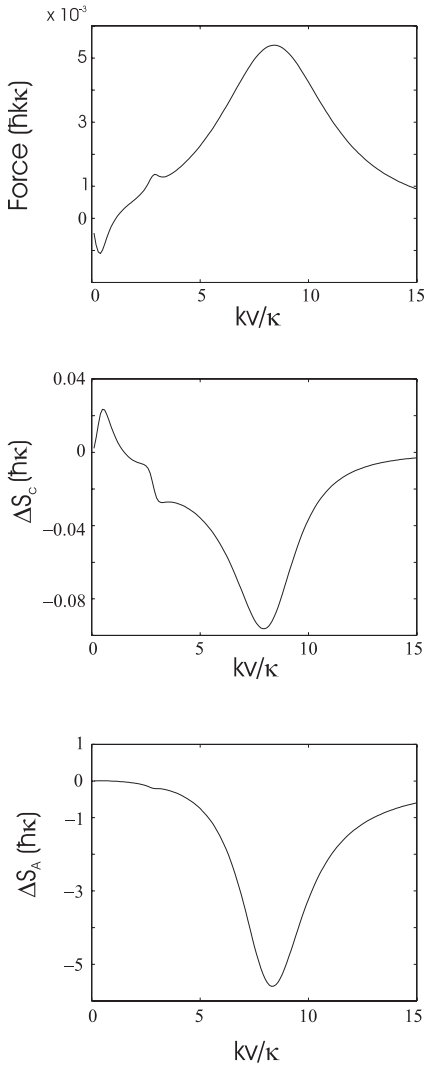

Fig. 21. Dipole force (upper picture), asymmetry in S_c (middle) and asymmetry in S_a. $\Delta_\mathrm{a} = 8\kappa$, $\Delta_\mathrm{c} = 0\kappa$, $g = 3\kappa$, $\Gamma = \kappa = 1$, $\eta = 0.1\kappa$.

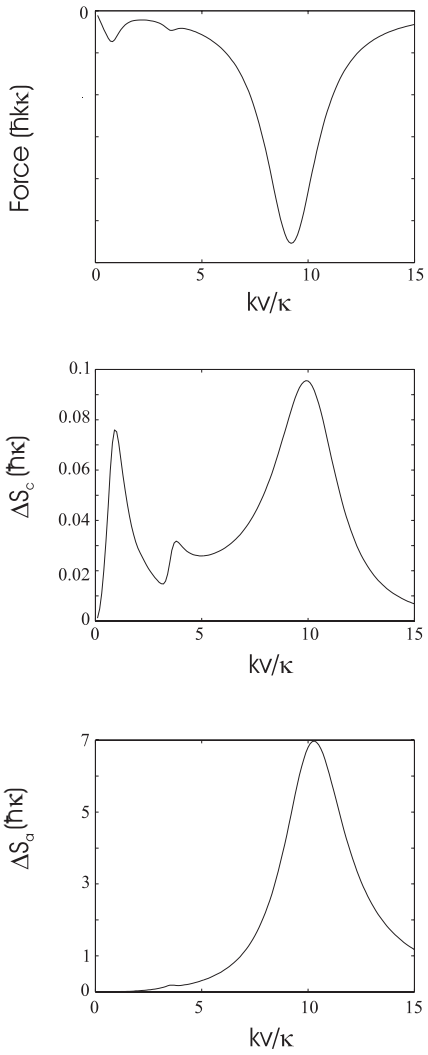

Fig. 22. Dipole force (upper picture), asymmetry in S_c (middle) and asymmetry in S_a. $\Delta_\mathrm{a} = -10\kappa$, $\Delta_\mathrm{c} = -2\kappa$, $g = 3\kappa$, $\Gamma = \kappa = 1$, $\eta = 0.1\kappa$.

gains falling a distance Δx, with the trapping potential change $\Delta U(x)$. In order to estimate the magnitude of the additional atomic acceleration we calculate the distance, for which the gravitational energy amounts to the recoil energy $E_\mathrm{R} = \hbar^2 k^2/2m$ of the atom absorbing or emitting a single photon. For Rb with an atomic mass of $85a_u$ one gets $\Delta x = 1700$ nm which corresponds to approximately 2λ ($\lambda = 780$ nm). As E_R is much smaller than $\hbar U_0 \approx \hbar\Gamma$ for most experimentally used atomic transitions, the influence of gravity should be rather small. However, for an atom falling transversely across the waist of the Gaussian mode ($w_0 \approx 100\lambda$), the gravitational potential energy can in fact get almost comparable to the trapping potential U_0. Consequently one should choose an experimental setup where the cavity axis is aligned along the direction of gravitational acceleration, if one is interested in a long time trapping of the atoms. In this way gravitational effects will not hamper the trapping process.

Several atoms moving simultaneously in the same mode will get motionally correlated and can also be trapped jointly at different nodes of the field. The consequences of the dynamics of one atom conditioned on the presence of a second atom in a given state could be thoroughly investigated in such systems. In comparison to linear ion traps the smallness of the cavity allows for a much stronger atom-field coupling, which strongly enhances the coherent part of the cavity mediated dynamics. Of course generalisations to even more atoms and especially a Bose-condensate inside the resonator mode look very promising. Similarily one could use higher order transverse modes to confine atoms to decoupled regions in the blue detuned case.

We thank G. Rempe, P. Pinske and P. Münstermann for helpful discussions. This work has been supported by the Austrian Fonds zur Förderung der wissenschaftlichen Forschung

under grant numbers S6506 and F1512 as part of the Spezialforschungsbereich Quantenoptik).

References

1. H. Mabuchi *et al.*, Opt. Lett. **21**, 1393 (1996).
2. G. Rempe, Appl. Phys. B **60**, 233 (1995).
3. P. Münstermann *et al.*, Opt. Commun. **159**, 63 (1999).
4. Q.A. Turchette, R.J. Thompson, H.J. Kimble, Appl. Phys. B **60**, S1 (1995).
5. D. Meschede, H. Walther, G. Mueller, Phys. Rev. Lett. **54**, 551 (1985); M. Brune *et al.*, Phys. Rev. Lett. **59**, 1899 (1987).
6. E.T. Jaynes, F.W. Cummings, Proc. IEEE **51**, 89 (1963).
7. J.P. Gordon, A. Ashkin, Phys. Rev. A **21**, 1606 (1980).
8. A.C. Doherty *et al.*, Phys. Rev. A **56**, 833 (1997).
9. K.S. Wong, M.J. Collett, D.F. Walls, Opt. Commun. **137**, 269 (1997).
10. P. Horak *et al.*, Phys. Rev. Lett. **79**, 4974 (1997).
11. G. Hechenblaikner *et al.*, Phys. Rev. A **58**, 3030 (1998).
12. A.C. Doherty *et al.*, Phys. Rev. A **57**, 4804 (1998).
13. J.-F. Roch *et al.*, Phys. Rev. Lett. **78**, 634 (1997)
14. K.S. Wong, M.J. Collett, D.F. Walls, Opt. Commun. **137**, 269 (1997).
15. J.A. Dunningham, H.M. Wiseman, D.F. Walls, Phys. Rev. A **55**, 1398 (1997).
16. K.M. Gheri, P. Horak, H. Ritsch , J. Mod. Opt. **44**, 605 (1997).
17. F. Haake *et al.*, Phys. Rev. Lett. **71**, 995 (1993).
18. A. Hemmerich (private communication).
19. R. Bonifacio *et al.*, in Coherent and Collective Interactions of Particles and Radiation Beams, *Proceedings of the International School of Physics "Enrico Fermi"*, Course CXXXI, edited by A. Aspect, W. Barletta, R. Bonifacio (IOS Press, Amsterdam, Oxford, Tokyo, Washington DC, 1996), pp. 285-323.
20. C. Cohen-Tannoudji, G. Grynberg, Opt. Commun. **96**, 150 (1993).
21. G. Morigi *et al.*, Phys. Rev. A (in press).
22. H.C. Nägerl *et al.*, Appl. Phys. B **66**, 603 (1998).
23. M. Löffler, G.M. Meyer, H. Walther, Europhys. Lett. **40**, 263 (1997).
24. W. Ren, J.D. Cresser, H.J. Carmichael, Phys. Rev. A **46**, 7162 (1992).
25. J.T. Höffges *et al.*, J. Mod. Opt. **44**, 1999 (1997).
26. J.H. Eberly, K. Wodkiewicz, J. Opt. Soc. Am. **67**, 1252 (1977).
27. C. Cohen-Tannoudji, in Fundamental Systems in Quantum Optics, *Proceedings of the Les Houches Summer School*, Session LIII, edited by J. Dalibard, J.-M. Raimond, J. Zinn-Justin (North-Holland, Amsterdam, 1992), pp. 1-164.